Delft University of Technology

# Chemo-mechanics of ageing on bituminous materials

Jing, Ruxin; Varveri, Katerina; Liu, Xueyan; Scarpas, Athanasios; Erkens, S.

**Publication date**
2018

**Document Version**
Accepted author manuscript

**Published in**
Transportation Research Board 97th Annual Meeting

**Citation (APA)**
Jing, R., Varveri, K., Liu, X., Scarpas, A., & Erkens, S. (2018). Chemo-mechanics of ageing on bituminous materials. In *Transportation Research Board 97th Annual Meeting : Washington DC, United States, 2018-1-7 to 2018-1-11*

**Important note**
To cite this publication, please use the final published version (if applicable).
Please check the document version above.

**Copyright**
Other than for strictly personal use, it is not permitted to download, forward or distribute the text or part of it, without the consent of the author(s) and/or copyright holder(s), unless the work is under an open content license such as Creative Commons.

**Takedown policy**
Please contact us and provide details if you believe this document breaches copyrights.
We will remove access to the work immediately and investigate your claim.

*This work is downloaded from Delft University of Technology.*
*For technical reasons the number of authors shown on this cover page is limited to a maximum of 10.*

**CHEMO-MECHANICS OF AGEING ON BITUMINOUS MATERIALS**

**Ruxin Jing (**Corresponding author)
Section of Pavement Engineering, Delft University of Technology
Stevinweg 1, Delft, the Netherlands, 2628 CN
Tel: + 31 (0)15 27 84674; Email: R.Jing@tudelft.nl

**Aikaterini Varveri**
Section of Pavement Engineering, Delft University of Technology
Stevinweg 1, Delft, the Netherlands, 2628 CN
Tel: + 31 (0)15 27 84665; Email: a.varveri@tudelft.nl

**Xueyan Liu**
Section of Pavement Engineering, Delft University of Technology
Stevinweg 1, Delft, the Netherlands, 2628 CN
Tel: + 31 (0)15 27 87918; Email: X.Liu@tudelft.nl

**Athanasios Scarpas**
Section of Pavement Engineering, Delft University of Technology
Stevinweg 1, Delft, the Netherlands, 2628 CN
Tel: + 31 (0)15 27 84017; Email: A.Scarpas@tudelft.nl

**Sandra Erkens**
Section of Pavement Engineering, Delft University of Technology
Stevinweg 1, Delft, the Netherlands, 2628 CN
Tel: + 31 (0)15 27 85949; Email: s.m.j.g.erkens@tudelft.nl

Word count: 4,000 words text + 14 tables/figures x 250 words (each) = 7,500 words

Submission Date: August 1, 2017

**ABSTRACT**

Ageing of bitumen is a complex process. It is accompanied by major chemical and mechanical changes. In this study, Fourier Transform Infrared (FTIR) spectrometer and Dynamic Shear Rheometer (DSR) tests were utilized to investigate the effect of ageing on the chemical and mechanical properties of bituminous materials. Bitumen films with thickness of 2 mm were exposed to laboratory ageing at various conditions. Specifically, different combinations of ageing time, temperature and pressure were applied on the materials. The FTIR tests results were used to quantify the changes in the chemical functional groups and to calculate ageing indices (carbonyl index and sulfoxide index) of bitumen. In addition, the DSR tests results were analysed to determine the evolution of the rheological properties of bitumen. A linear relationship was made between the ageing indices and complex shear modulus, providing thus a chemo-mechanics framework to describe bitumen ageing. The results were validated by using data of field aged samples. Finally, the influence of ageing on the parameters of two viscoelastic models was determined.

*Keywords*: Bitumen, Ageing, FTIR Spectroscopy, Rheology, Chemo-mechanics model

# INTRODUCTION

In the Netherlands, the short service life of porous asphalt pavements due to ravelling is a major concern. Ageing of bituminous materials is believed to be one of the major causes. The mechanical and chemical properties of bitumen, as of all organic substances, evolve with time. It is well known that as bitumen ages its ductility and penetration index are reduced while the softening point is increased (*1-3*). Ultimately, the viscosity of the bitumen is increased and bitumen becomes stiffer. This may cause the mixture to become excessively brittle and susceptible to fatigue damage and cracking at lower temperatures (*4*).

In the past, research has shown that typical bitumen properties such as viscosity, penetration, softening point and ductility had a good correlation with ageing (*5-7*). At that time the level of ageing was expressed as a reduction in penetration, an increase in softening point or as the ratio of viscosities, always in relation with the unaged (fresh) condition (*8*, *9*). Based on large datasets of recovered bitumen from the field, several empirical models were reported to predict the long-term performance of bituminous materials (*10-12*).

Recently, more and more researchers attempted to correlate the chemical composition of bituminous materials with their performance (*13*, *14*). Studies have indicated that the ageing mechanism affects the chemical composition of bitumen and it was clear that the rheological properties would change as well (*15-18*). Unfortunately, the specific relationship between the chemical properties and mechanical response of bitumen is still unclear. If this relationship is established, then predictions of pavement performance over longer time periods can be made possible.

# OBJECTIVES

The main objective of this study is to determine the changes in the chemical properties of bitumen due to ageing and link them to its mechanical response, by means of Fourier Transform infrared (FTIR) spectrometer and Dynamic Shear Rheometer (DSR) tests. For this, bitumen films were aged in the laboratory at various times, temperatures and pressures. On the basis of the experimental results, a chemo-mechanics ageing theory is developed and validated using results of field aged samples. Finally, another objective is to determine the influence of ageing on the parameters of the viscoelastic models.

# MATERIALS AND AGEING METHOD

## Materials

The PEN 70/100 bitumen, which is one of the most commonly used in Netherlands, was used in this study. Table 1 shows the main physical and rheological properties of the examined bitumen. The same bitumen type was used for the construction of test sections that were used for bitumen recovery as explained in the following sections.

**TABLE 1 Specifications of PEN 70/100 at Fresh (Unaged) State**

| **Property** | **Unit** | **PEN 70/100** |
|---|---|---|
| Penetration at 25 °C | 0.1 mm | 70-100 |
| Softening point | °C | 43-51 |
| Dynamic viscosity at 60 °C | Pa s | 160 |
| Complex shear modulus at 1.6 Hz & 60 °C | kPa | 1.8 |
| Phase angle at 1.6 Hz & 60 °C | ° | 88 |

## Laboratory ageing

In this study, bitumen films with 2 mm thickness were aged by two different ageing methods: oven ageing and PAV (Pressure Ageing Vessel) ageing. Oven ageing was applied for various ageing time and temperatures, while PAV ageing was applied for various ageing pressures. Table 2 summarizes the various ageing processes that were considered.

**TABLE 2 Ageing Program**

| Ageing Method | Temperature (°C) | Pressure (atm) | Ageing Time (h) |
|---|---|---|---|
| Oven | 100 | 1 | 20, 40, 80, 160, 320 |
| Oven | 50, 150 | 1 | 40 |
| PAV | 100 | 5, 10, 15, 20 | 40 |

**Field ageing**

The same PEN 70/100 bitumen was used for the construction of test sections. The pavement sections have been constructed in October 2014 and are continuously exposed to the various environmental conditions. The pavement structure is shown in Figure 1. The top layer is porous asphalt concrete (PAC), which is widely used in Netherlands.

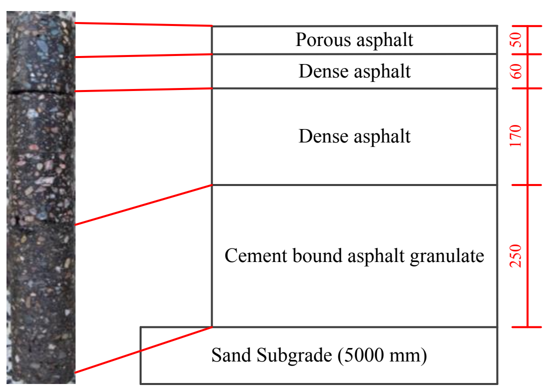


**FIGURE 1 Structure of field test section (length unit: mm).**

Asphalt cores (diameter is 10 mm) were taken from the PAC layer every year until now. Then the samples were cut into three slices (each slice with 12~14 mm thickness), so that the ageing development at the depth profiles of the pavement can be studied. Then, the chemical and rheological properties of extracted bitumen from the different slices was evaluated.

## EXPERIMENTAL METHOD

In order to relate the changes in chemical behaviour of the bitumen due to oxidative ageing with the mechanical responses of the material, FTIR and DSR test methods were employed for evaluating the changes in the chemical and rheological properties of bitumen.

**Fourier Transform Infrared spectrometer**

The tests were performed using the Spectrum 100 FT-IR spectrometer of Perkin-Elmer available at the Section of Pavement Engineering in TU Delft. A single-beam configuration was used. The sample was scanned 20 times, with a fixed instrument resolution of 4 $cm^{-1}$. The wavenumbers was set to vary from 600 to 4000 $cm^{-1}$.

The chemical composition of bitumen is very complex, therefore specific peaks at selected wavenumbers were used to investigate the changes in the functional groups due to bitumen ageing. In this study, the effects of ageing were studied considering specific bands of wavenumber and the corresponding area under those bands. Using the area values, the ageing indices were calculated. The characteristic regions were adopted from a previous study (*17*). The most important infrared region is between wavenumbers of 1800-600 $cm^{-1}$. This area provides information about the functional chemical groups which contain oxidation products such as carbonyls (1753-1660 $cm^{-1}$) and sulfoxides (1047-995 $cm^{-1}$). This region is also called the fingerprint region. The functional groups that are normally used to characterize the effects of ageing on bitumen chemistry are summarized in Table 3.

**TABLE 3 Vertical Limit Bands with the Corresponding Functional Groups**

| **Area** | **Vertical Band Limit ($cm^{-1}$)** | **Functional Groups** |
|---|---|---|
| $A_{724}$ | 734-710 | Long chains |
| $A_{743}$ | 783-734 | Out of plane adjacent |
| $A_{814}$ | 838-783 | Out of plane adjacent |
| $A_{864}$ | 912-838 | Out of plane singlet |
| $A_{1030}$ | 1047-995 | Oxygenated functions - sulfoxide |
| $A_{1376}$ | 1390-1350 | Branched aliphatic structures |
| $A_{1460}$ | 1525-1395 | Aliphatic structures |
| $A_{1600}$ | 1670-1535 | Aromatic structures |
| $A_{1700}$ | 1753-1660 | Oxygenated functions - carbonyl |
| $A_{2862}$ | 2880-2820 | Stretching symmetric |
| $A_{2953}$ | 2990-2880 | Stretching aromatic |

On the basis of these bandwidths the ageing indices, carbonyl and sulfoxide index were calculated. The calculation is performed by dividing the area under a specific location of the spectrum by the sum of others specific areas. The analytical expressions to determine the ageing indices are shown in Equations (1) to (3).

$$\text{Carbonyl index} = \frac{A_{1700}}{\sum A} \quad (1)$$

$$\text{Sulfoxide index} = \frac{A_{1030}}{\sum A} \quad (2)$$

$$\sum A = A_{(2953,2862)} + A_{1700} + A_{1600} + A_{1460} + A_{1376} + A_{1030} + A_{864} + A_{814} + A_{743} + A_{724} \quad (3)$$

**Dynamic Shear Rheometer**

DSR tests were performed at the Section of Pavement Engineering in TU Delft. The bitumen samples were tested using the parallel-plates configuration. Initially, the linear viscoelastic (LVE) strain range of bitumen samples was determined using amplitude sweep tests. The frequency sweep tests were performed at five different temperatures (0, 10, 20, 30 and 40 °C). During the tests the frequency varied in a logarithmic manner from 50 Hz to 0.01 Hz. At least three repetition tests were done for each ageing condition.

The complex shear modulus and phase angle values were collected during the tests. Master curves were constructed, in order to determine the visco-elastic behaviour in a wider range of frequencies. In this study, the reference temperature was selected as 20 °C.

## RESULTS AND DISCUSSION

**Fourier Transform Infrared spectrometer**

Bitumen samples subjected to different ageing conditions were tested by means of FTIR. At least three replicate samples were tested at each condition. Figure 2 shows the FTIR spectra with wavenumbers less than 2000 $cm^{-1}$ at various ageing conditions. This wavenumbers correspond to functional groups related to the oxidation processes.

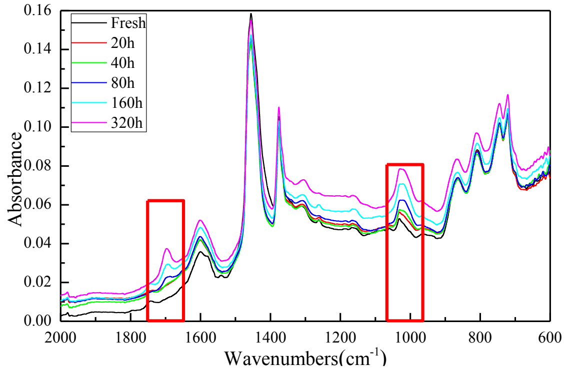


(a) Different ageing time (oven ageing at 100 °C and 1 atm).

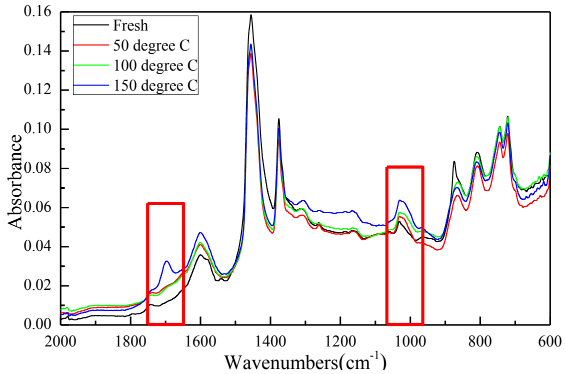


(b) Different ageing temperatures (oven ageing for 40 h at 1 atm).

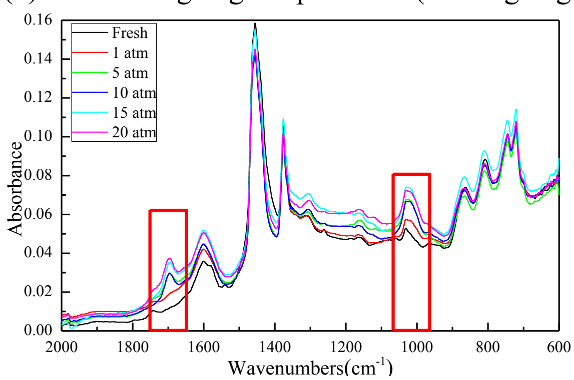


(c) Different ageing pressures (PAV ageing for 40 h at 100 °C).

**FIGURE 2 Detail of the FTIR spectra of PEN 70/100 at different ageing conditions.**

Figure 2 shows the high variability of the carbonyl (left red part) and sulfoxide (right red part) functional groups. They are both increased with increasing ageing time (Figure 2 (a)), temperature (Figure 2 (b)) and pressure (Figure 2 (c)). Figure 3 shows the carbonyl and sulfoxide indices (average value of three measurements), which were calculated based on Equation (1) to (3).

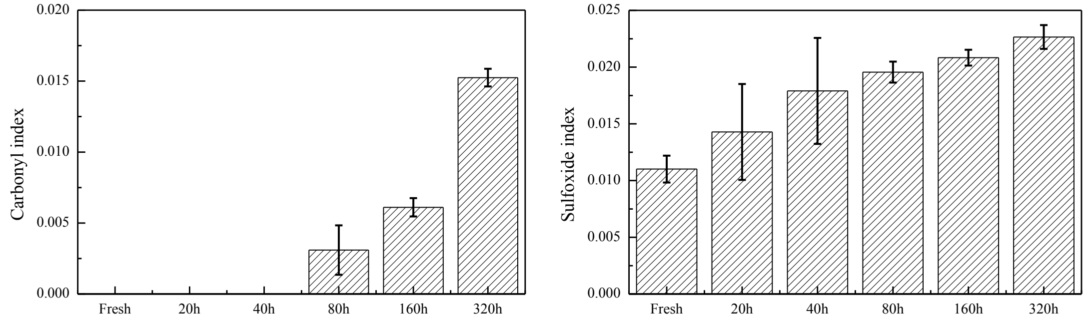


(a) Different ageing time (oven ageing at 100 °C and 1 atm).

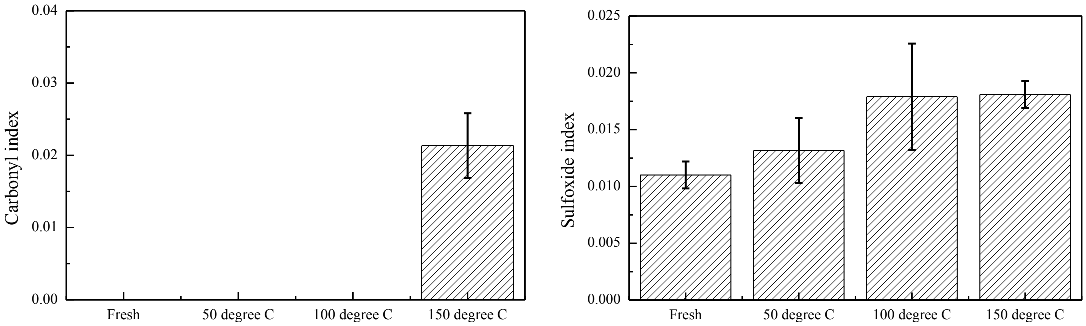


(b) Different ageing temperatures (oven ageing for 40 h at 1 atm).

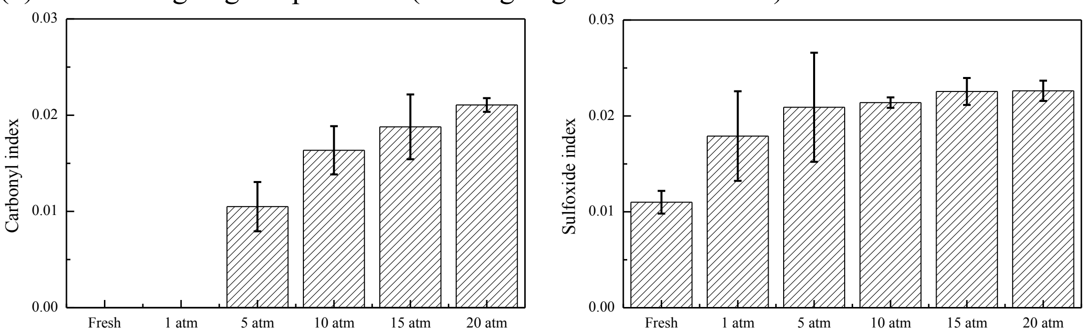


(c) Different ageing pressures (PAV ageing for 40 h at 100 °C).

**FIGURE 3 Ageing indices of PEN 70/100 at different ageing conditions.**

The results showed that, oven ageing at 100 °C and 1 atm causes an increase of the sulfoxide index with time. It is interesting to note that carbonyls start forming after 40 hours ageing and then increase with time, while the sulfoxide index increases slightly. Figure 3(b) shows that, the sulfoxide index increases with ageing temperature (at 1 atm and 40 hours), while no carbonyls are formed below 100 °C. When temperature exceeds 100 °C the carbonyl index increases with ageing temperature, whereas the sulfoxide index remains stable. On the other hand, ageing pressure was observed to stimulate the formation of carbonyl compounds. Figure 3(c) shows that the sulfoxide index increases with ageing pressure, while no carbonyls are formed below 1 atm. Above 1 atm the carbonyls index increases with ageing pressure, in contrast the sulfoxide index shows no change in its value.

In summary, sulfoxides are formed earlier than carbonyls, because sulfur is more reactive than carbon in bitumen. The results show that only sulfoxides are formed, and further increase, under weak ageing conditions (short ageing time, low ageing temperature and pressure), while no (or few) carbonyls are formed. On the contrary, carbonyls increase under strong ageing conditions (long ageing time, high ageing temperature and pressure), whereas the sulfoxide index is stable probably due to the full consumption of sulfur.

**Dynamic Shear Rheometer**

The bitumen samples after the application of different ageing conditions were also tested by means of the DSR. At least three replicate samples were tested at each condition. Based on the TTS principle, master curves of complex shear modulus and phase angle were generated at reference temperature 20 °C. Figure 4 shows the evolution of the rheological characteristics of bitumen with increased ageing time, temperature and pressure.

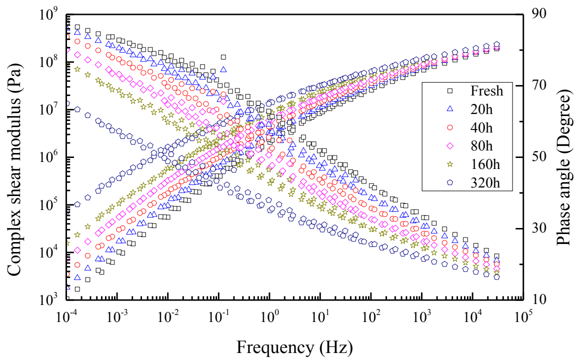


(a) Different ageing time (oven ageing at 100 °C and 1 atm).

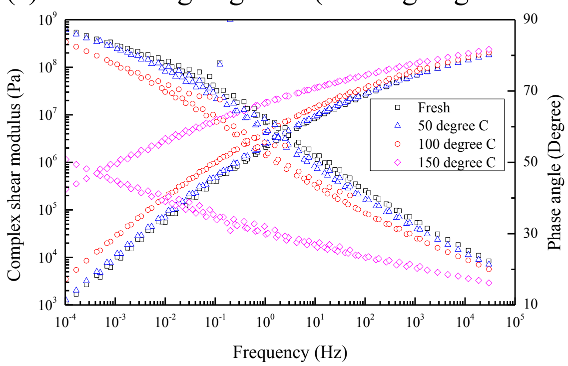


(b) Different ageing temperatures (oven ageing for 40 h at 1 atm).

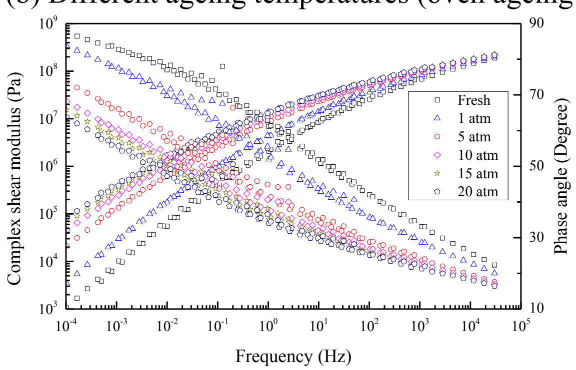


(c) Different ageing pressures (PAV ageing for 40 h at 100 °C).

**FIGURE 4 Master curves of PEN 70/100 at different ageing conditions.**

In Figure 4, the observed differences are more pronounced at low frequencies, while they dilute at higher frequencies at which the materials behave more elastic. Specifically, the variation of complex modulus between fresh and aged materials was about two orders of magnitude at low frequencies. Moreover, at the highest frequency, all samples tend to reach an asymptote at a value of $10^8$ Pa. On the contrary, the phase angle differs substantially for the whole frequency range. Comparing (a), (b) and (c), it can be observed that temperature is the most influential parameters for ageing, probably because of the fact that the ageing rate coefficient increases exponentially with temperature based on the Arrhenius equation (*18*).

## CHEMO-MECHANICS OF AGEING MODEL

### Model development

Figure 5 illustrates plots of the carbonyl index, sulfoxide index and their summation with increasing ageing time, Figure 5(a), temperature, Figure 5(b), and pressure, Figure 5(c). Also, the complex shear moduli at 10 Hz and 20 °C are plotted on the right hand side of Figure 5 right column. Each point in the graph represents the average value of three replicate samples.

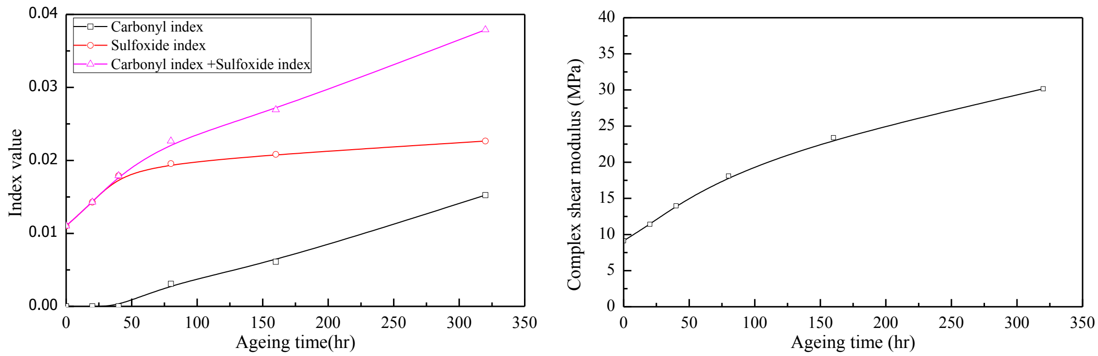


(a) Different ageing time (oven ageing at 100 °C and 1 atm).

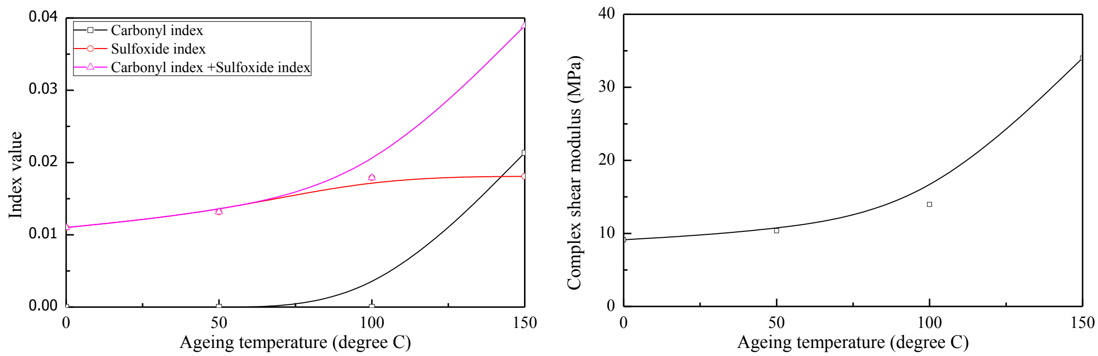


(b) Different ageing temperatures (oven ageing for 40 h at 1 atm).

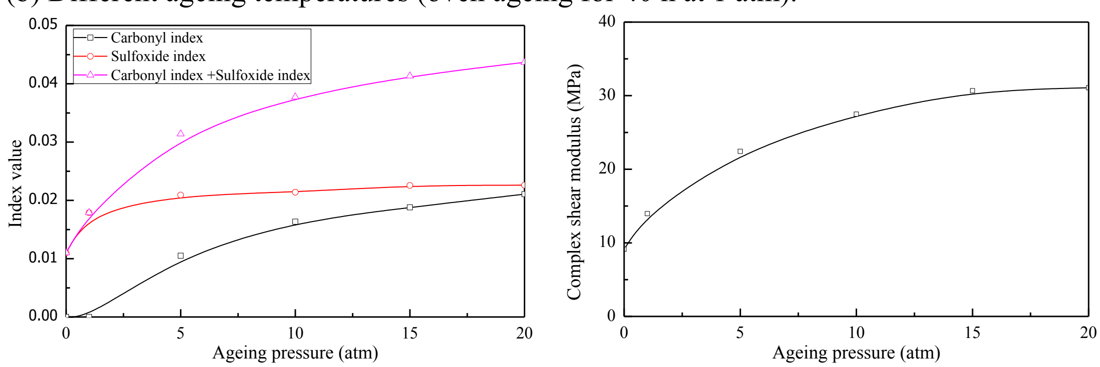


(c) Different ageing pressures (PAV ageing for 40 h at 100 °C).

**FIGURE 5 Ageing indices (left column) and complex shear moduli at 20 °C and 10Hz (right column) of PEN 70/100 at different ageing conditions.**

For each ageing condition, the relationship between chemical and mechanical properties of aged bitumen can be described by using a combined ageing index (carbonyl index + sulfoxide index) and the value of the complex shear modulus (at 10 Hz, 20 °C). Figure 6 shows that there is a linear relationship between the ageing index and the complex shear modulus of aged bitumen. It is interesting to note that this relationship does not depend on the ageing methods. In another words, different ageing conditions can be interrelated with each other.

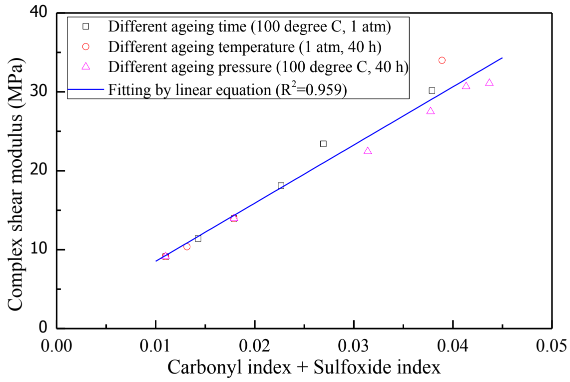


**FIGURE 6 Complex shear modulus at 10 Hz, 20 °C vs the summation of the carbonyl and sulfoxide indices at different ageing conditions.**

## Model validation

In order to correlate laboratory ageing to field ageing, bitumen was extracted from the pavement test sections and tested for its rheological and chemical properties.

Following the aforementioned methodology, the relationship between the combined ageing index (carbonyl index + sulfoxide index) and the complex shear modulus (10 Hz, 20 °C) was found. The results after laboratory and field ageing are plotted in Figure 7. The black points in the graph are the results from the laboratory aged samples and the coloured symbols are from field aged samples.

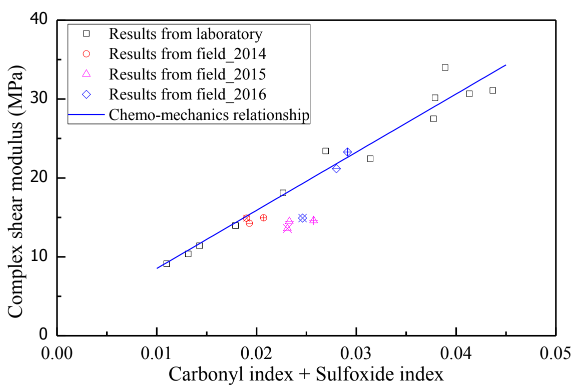


**FIGURE 7 Comparison of laboratory and field results.**

Considering the test error, Figure 7 shows an overall agreement between field results and the predictions of the chemo-mechanics of ageing model. Furthermore, for the field results, the symbols with '+', '-' and 'x' correspond to the results of bitumen samples from top, middle and bottom slices respectively. It can be observed that the effect of ageing is more pronounced on the top of the pavement and decreases with increasing pavement depth. Also, the differences in ageing among the three depths increase with ageing time.

## AGEING EFFECT ON CONSTITUTIVE MODEL

### CAM Model

The results of master curves for the complex shear modulus and the phase angle are described by the CAM model as

$$G^*(f) = G_e^* + \frac{G_g^* - G_e^*}{\left[1+\left(f_c/f\right)^k\right]^{m/k}} \tag{4}$$

$$\delta(f) = \delta_e + \frac{\delta_g - \delta_e}{\left[1+\left(f_d/f\right)^k\right]^{m/k}} \tag{5}$$

where $G_e^*$ and $\delta_e$ are the complex shear modulus and the phase angle, respectively, when $f \to 0$. Similarly, $G_g^*$ and $\delta_g$ are the complex shear modulus and the phase angle, respectively, when $f \to \infty$. Also, $f_c$ and $f_d$ are position frequencies for the master curve of complex shear modulus and phase angle, respectively, and $m$ and $k$ are fitting parameters. Figure 8 (a) gives a good description of each term in CAM model. For the bituminous materials it can be assumed that $G_e^* = 0$, $\delta_e = 90^\circ$ and $\delta_g = 0^\circ$.

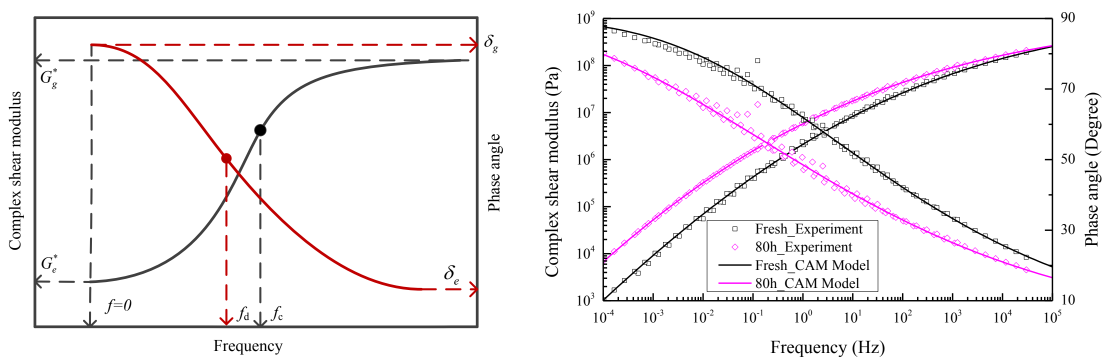


(a) Schematic of model response (b) Model validation

**FIGURE 8 CAM model.**

The master curves (reference temperature is 20 °C) of the complex shear modulus and phase angle were fitted to the CAM model using Equation (4) and (5). All model parameters can be obtained by minimizing the mean relative error, as defined in Equation (6).

$$MRE = \sum \frac{\left|G_c^* - G_t^*\right|}{G_t^*} + \sum \frac{\left|\delta_c - \delta_t\right|}{\delta_t} \tag{6}$$

where $MRE$ is the mean relative error, $G_c^*$ is the calculated value and $G_t^*$ is the test value of complex shear modulus, $\delta_c$ is the calculated value and $\delta_t$ is the test value of the phase angle. The model parameters are presented in Table 4, where the Ageing Index is the summation of the carbonyl and the sulfoxide indices. From Table 4, a difference between the fresh and the aged materials can be clearly observed. Specifically, at higher frequencies corresponding to lower temperature, the absolute value of the complex modulus $G_g^*$ increases to some extent with increasing ageing time, temperature or pressure. However, the differences are not significant and it can be anticipated that the glassy modulus at $f \to \infty$ will converge to a threshold value irrespective of the ageing conditions. On the other hand, ageing causes a shift in the $G^*$ and $\delta$ master curves to the left as demonstrated by the decay of the $f_c$ and $f_d$ values, Table 4. This shift results in higher complex modulus and lower phase angle values, which is indicative of bitumen embrittlement with ageing.

The model was validated using two sets of data, at fresh (unaged) conditions and after 80hrs of oven ageing at 100°C. The results show, Figure 8 (b), that the model is able to capture the response of the materials across the frequency spectrum.

**TABLE 4 CAM Model Fitting Parameters**

| **Ageing Condition** | | | **CAM Model Parameters** | | | | | | **Ageing Index** |
|---|---|---|---|---|---|---|---|---|---|
| t (h) | T (°C) | P (atm) | $G_g^*$ (GPa) | $f_c$ (Hz) | $f_d$ (Hz) | $k$ | $M$ | $MRE$ | |
| Fresh | | | 1.46 | 1.96 | 8.23E-07 | 0.14 | 1.23 | 7.13 | 0.010 |
| 20 | 100 | 1 | 1.49 | 0.27 | 3.65E-08 | 0.13 | 1.34 | 5.26 | 0.014 |
| 40 | 100 | 1 | 1.42 | 0.05 | 2.66E-09 | 0.13 | 1.41 | 4.26 | 0.018 |
| 80 | 100 | 1 | 1.34 | 3.12E-03 | 4.51E-11 | 0.12 | 1.57 | 3.82 | 0.023 |
| 160 | 100 | 1 | 1.45 | 6.52E-04 | 2.25E-12 | 0.11 | 1.61 | 4.11 | 0.027 |
| 320 | 100 | 1 | 1.59 | 1.64E-04 | 4.52E-17 | 0.10 | 1.86 | 5.18 | 0.038 |
| 40 | 50 | 1 | 1.25 | 0.77 | 2.73E-07 | 0.14 | 1.28 | 5.43 | 0.013 |
| 40 | 150 | 1 | 1.47 | 4.51E-08 | 1.99E-22 | 0.08 | 1.62 | 5.39 | 0.039 |
| 40 | 100 | 5 | 1.38 | 1.01E-04 | 1.03E-13 | 0.11 | 1.71 | 4.77 | 0.035 |
| 40 | 100 | 10 | 1.44 | 6.23E-06 | 5.93E-16 | 0.10 | 1.82 | 5.00 | 0.038 |
| 40 | 100 | 15 | 1.50 | 1.44E-06 | 5.49E-17 | 0.10 | 1.90 | 5.61 | 0.041 |
| 40 | 100 | 20 | 1.50 | 7.72E-07 | 1.04E-17 | 0.09 | 1.87 | 6.00 | 0.042 |

**Generalized Maxwell Model**

Figure 9(a) shows the schematic of the Generalized Maxwell (GM) viscoelastic model. The constitutive equation of the GM model is defined as

$$\sum_{k=0}^{n} p_k \frac{d^k \sigma}{dt^k} = \sum_{k=0}^{n} q_k \frac{d^k \varepsilon}{dt^k} \tag{7}$$

where $p_k$ and $q_k$ are material parameters. Under sine loading, the storage modulus, the loss modulus, the complex shear modulus and the phase angle can be written as

$$G'(f) = \sum_{i=1}^{m} \frac{G_i f^2 \rho_i^2}{1 + f^2 \rho_i^2} \tag{8}$$

$$G''(f) = \sum_{i=1}^{m} \frac{G_i f \rho_i}{1 + f^2 \rho_i^2} \tag{9}$$

$$G^*(f) = \sqrt{\left(G'(f)\right)^2 + \left(G''(f)\right)^2} \tag{10}$$

$$\delta = \arctan \frac{G''(f)}{G'(f)} \tag{11}$$

where $\rho_i = \frac{\eta_i}{G_i}$, $G_i$ and $\eta_i$ is the shear modulus and the viscosity of $i^{th}$ Maxwell element.

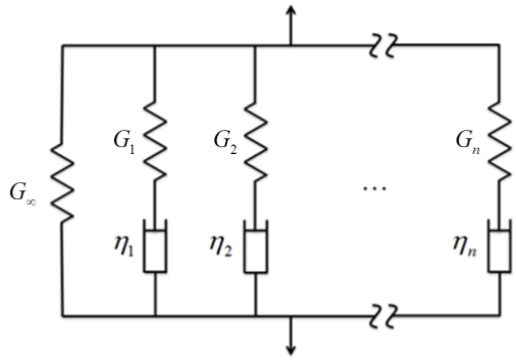


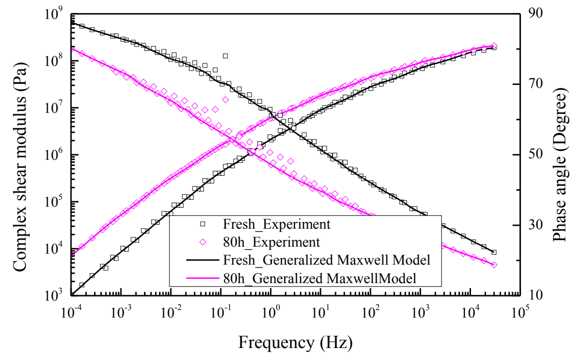


(a) Schematic (b) Model validation

**FIGURE 9 Generalized Maxwell model.**

In this study, a GM model with 10 parallel Maxwell components was selected to fit the master curve of the complex shear modulus and the phase angle at a reference temperature of 20 °C. The value of $\rho_i$ was selected to vary from $10^{-4}$ to $10^5$. $G_\infty = 0$ was chosen. The additional model parameters were obtained by minimizing the mean relative error as shown in Equation (6). The results are presented in Figure 10 and the validation of the model for two sets of data is shown in Figure 9 (b).

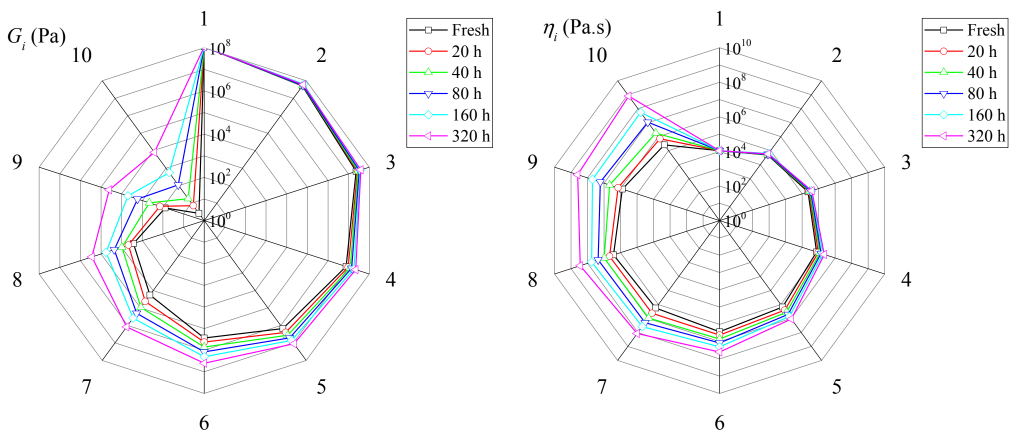


(a) The influence of various ageing times on shear modulus $G_i$ and viscosity $\eta_i$ (oven ageing at 100 °C and 1 atm).

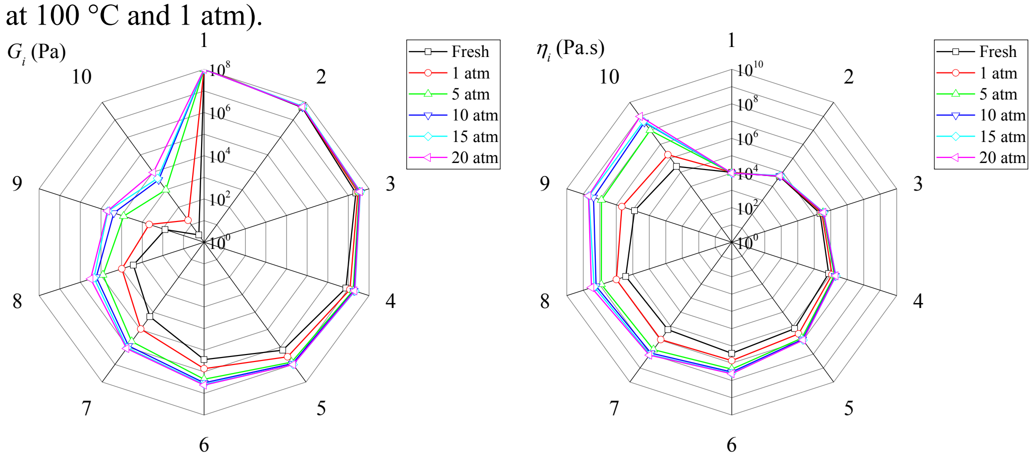

(b) The influence of various ageing temperatures on shear modulus $G_i$ and viscosity $\eta_i$ (oven ageing for 40 h at 1 atm).

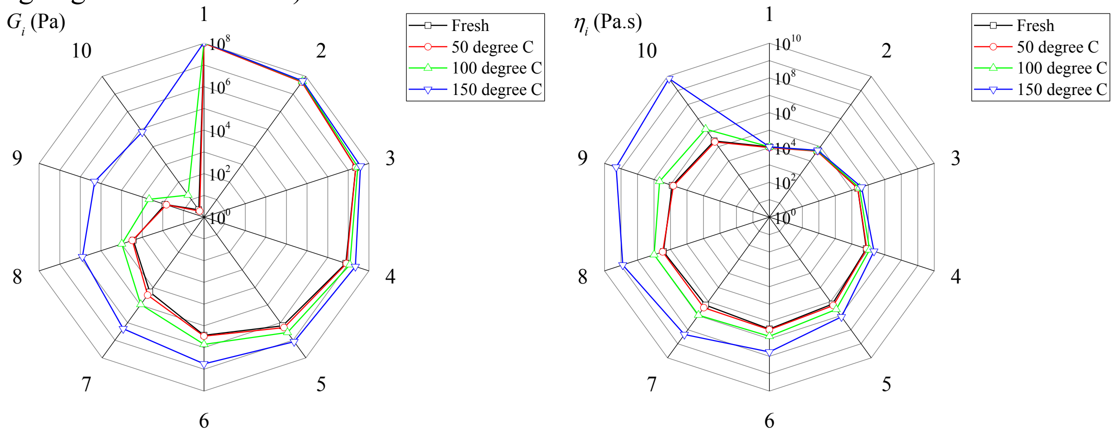


(c) The influence of various ageing pressures on shear modulus $G_i$ and viscosity $\eta_i$ (PAV ageing for 40 h at 100 °C).

**FIGURE 10 Shear modulus $G_i$ and viscosity $\eta_i$ of each Maxwell element component at different ageing conditions.**

Figure 10 shows that ageing affects in a greater degree the more viscous Maxwell element, with longer characteristic relaxation times $\rho_i$, at unaged conditions. It can be observed that both the complex shear modulus and viscosity increase as bitumen is subjected to longer ageing times as well as higher temperature or pressure. However, it is no unusual to observe larger differences in the values of complex shear modulus at lower testing frequencies or equivalently higher temperature, at which the viscous component dominates bitumen behavior.

## CONCLUSIONS

Given the strong relationship between the mechanical pavement response and ageing, which is a chemically-induced process, the knowledge of the evolution of the chemical properties in bituminous materials is of uppermost importance. For this reason, a series of ageing experiments were conducted on 2 mm thickness bitumen films at different times, temperatures, and pressures.

In order to develop a chemo-mechanics model of ageing, a series of FTIR and DSR tests were carried out to determine the changes in chemical properties and rheological response of aged bitumen. A linear relationship was found to exist between the complex shear modulus (10 Hz, 20 °C) and the combined ageing index (carbonyl index + sulfoxide index). The measured chemo-mechanic relationships from laboratory aged samples were in good correspondence with the results of field aged samples. The chemo-mechanics model of ageing clearly confirms the well-known fact that different ageing conditions can yield the same ageing effect.

Two typical constitutive models were selected and the influence of ageing was studied. For the CAM model, the complex shear modulus at infinite frequency increases slightly with ageing. However, both the complex shear modulus and the phase angle position frequencies decrease with ageing. For the Generalized Maxwell model, ageing was observed to influence more on the more viscous Maxwell elements.

As a continuation of this research, the same methodology will be used to develop a chemo-mechanics model of ageing for mastics and mortars. Meanwhile, finite element simulations will be performed to demonstrate the influence of ageing on the chemical properties and on the mechanical response of bituminous materials.

## ACKNOWLEDGMENTS

The authors gratefully acknowledge the Dutch Ministry of Transport, Public Works and Water Management for funding this project.

## REFERENCES

1. Lesueur, D. The Colloidal Structure of bitumen: Consequences on the Rheology and on the Mechanisms of Bitumen Modification. *Advances in Colloid and Interface Science*, Vol. 145, 2009, pp. 42-82. https://doi.org/10.1016/j.cis.2008.08.011
2. Siddiqui, M. N., and M. F. Ali. Investigation of Chemical Transformations by NMR and GPC During the Laboratory Aging of Arabian Asphalt. *Fuel*, Vol. 78, 1999, pp. 1407-1416. https://doi.org/10.1016/S0016-2361(99)00080-0
3. Saoula, S., Soudani, K., Haddadi, S., Munoz. M., and A. Santamaria, Analysis of the Rheological Behavior of Aging Bitumen and Predicting the Risk of Permanent Deformation of Asphalt. *Materials Sciences and Applications*, Vol. 4, No. 5, 2013, pp. 312-318. http://dx.doi.org/10.4236/msa.2013.45040
4. Kliewer, J. E., C. A. Bell, and D. A. Sosnovske, Investigation of the Relationship Between Field Performance and Laboratory Aging Properties of Asphalt Mixtures. *Engineering Properties of Asphalt Mixtures and the Relationship to Their Performance*, ASTM International, West Conshohocken, PA, 1995, pp. 3-20. https://doi.org/10.1520/STP15559S
5. Doye, P. C., Creaking Characteristic of Asphalt Cement. *Association of Asphalt Paveing Technology*, Vol. 27, 1958, pp. 581-597.
6. Vallerga, B. A., and W. J. Halstead, Effect of Field Ageing on Fundamental Properties of Pavement Asphalts. 50th Annual Meeting of the Highway Research Board, Washington, D. C., 1971, pp. 71-92.
7. Kandhal, P. S., and W. C. Koehler, Significant Studies on Asphalt Durability: Pennsylvania Experience. *Transportation Research Record*: *Journal of the Transportation Research Board*, No. 999, 1984, pp. 41-50.
8. Rostler, F. S. and R. M. White, Influence of Chemical Composition of Asphalts on Performance, Particularly Durability. *Symposium on Road and Paving Materials*, ASTM International, West Conshohocken, PA, 1960, pp. 64-88. https://doi.org/10.1520/STP38773S
9. Petersen, J. C., A Thin Film Accelerated Aging Test for Evaluating Asphalt Oxidative Aging. *Association of Asphalt Paving Technologist Proc*, Vol. 58, 1989, pp. 220-237.
10. Kumar, A., and W. H. Goetz. Asphalt Hardening as Affected by Film Thickness, Voids and Permeability in Asphaltic Mixtures. *Association of Asphalt Paving Technologists Proc*, Vol. 46, 1977, pp.571-605.
11. Shahin, M. Y., Design System for Minimizing Asphalt Concrete Thermal Cracking. *4th International Conference on Structural Design of Asphalt Pavements*, Ann Arbor, Michigan, Vol. 1, 1977, pp. 920-932.
12. Dauzats, M. and A. Rampal, Mechanism of Surface Cracking in Wearing Courses. *6th International Conference, Structural Design of Asphalt Pavements*, Ann Arbor, Michigan, Vol. 1, 1987, pp. 232-247.

13. Petersen, J. C. and R. Glaser, Asphalt Oxidation Mechanisms and the Role of Oxidation Products on Age Hardening Revisited. *Road Materials and Pavement Design*, Vol. 12, 2011, pp. 795-819. http://dx.doi.org/10.1080/14680629.2011.9713895

14. Lu, X. and U. Isacsson, Effect of Ageing on Bitumen Chemistry and Rheology. *Construction and Building Materials*, Vol. 16, 2002, pp. 15-22. https://doi.org/10.1016/S0950-0618(01)00033-2

15. Petersen, J. C., Chemical Composition of Asphalt as Related to Asphalt Durability: State of the Art. *Transportation Research Record: Journal of the Transportation Research Board*, No. 999, 1984, pp.13-30.

16. Herrington, P. R., J. E. Patrick, and G. F. Ball, Oxidation of Roading Asphalts. *Industrial & Engineering Chemistry Research*, 1994, pp. 2801-2809. https://doi.org/ 10.1021/ie00035a033

17. Glaser R. R., Turner T. F., Loveridge J. L. Salmans S. L. and Planche J. P. Ageing Master Curve and Ageing Rate Model, *Technical White Papers of WRI*, 2015

18. Boysen R. and Schabron J., Laboratory and Field Asphalt Binder Aging: Chemical Changes and Influence on Asphalt Binder Embrittlement, *Technical White Papers of WRI*, 2015

19. W. Van den bergh, *The Effect of Ageing on the Fatigue and Healing Properties of Bituminous Motars*, Delft, the Netherlands, 2011.

20. Glaser R. R., J. F. Schabron, T. F. Turner, J. P. Planche, S. L. Salmans, and J. L. Loveridge. Low-Temperature Oxidation Kinetics of Asphalt Binders. *Transportation Research Record: Journal of the Transportation Research Board*, No. 2370, 2013, pp. 63-68. http://dx.doi.org/10.3141/2370-08



View publication stats